Sensors for active control of turbulent combustion

L.Zimmer[1], S. Tachibana[1], M. Tanahashi[2], M. Shimura[2] and T. Miyauchi[2]

[1]*Japan Aerospace Exploration Agency*
7-44-1 Jindaiji-Higashi, Chofu, Tokyo, 182-8522 Japan

[2]*Department of Mechanical and Aerospace Engineering, Tokyo Institute of Technology*
2-12-1 Ookayama, Meguro-ku, Tokyo, 152-8522, Japan

E-mail: zimmer.laurent@jaxa.jp

Abstract

The purpose of this article is to describe two sensors readily available for active control of combustion and to show their different possibilities. The first one concerns the chemiluminescence measurements, both spectrally and temporally resolved. It is shown that the adjunction of secondary fuel injection leads to an increase in the relative C_2* emission, which is a mark of rich flames and therefore that the injected fuel is not burning in a premixed mode. Phase-locked measurements enable also a description of the oscillations, as seen by chemiluminescence. It is shown that the ratio OH*/CH* fluctuates strongly for non-controlled cases but remains stable for controlled cases. The control clearly aims at damping the oscillations of this ratio. Looking at spectra of time resolved chemiluminescence reveals similar results than that of pressure, however some features are enhanced which may be a source for further improvement of the active control. To realize the active combustion control, diode-laser absorption sensor has been developed. It is shown that the diode-laser absorption sensor can measure the high frequency fluctuation of temperature and mole fraction of H_2O in the burned gas at the exit of the combustor. The r. m. s. of measured properties and power spectra well reflect characteristics of the combustor such as noise level, and the measured peak frequency coincide with those of the pressure fluctuation in the combustor. These results suggest that the diode-laser absorption sensor is a strong candidate of a sensor for the active combustion control. Both techniques are described and compared with typical output of pressure sensors to illustrate the common points as well as the extra information gained.

1. General introduction

Reducing pollutant emission is becoming a major issue for many industrial applications. It is known that using premixed combustion is favorable in terms of pollutant emission, compared to non-premixed systems. However, the main disadvantage of the premixed combustion is that oscillations are very easy to get. Therefore, one has to look for strategies to suppress those instabilities: this is the role of Active Control of Combustion (ACC). ACC requires information from the dynamics of the combustion system to be used as input in the control loop (Candel, 2002). The system will be modified and the modifications induced measured until the desired operating point is achieved. The main problem lies in the determination of the actual conditions within the combustor. Quantitative diagnostics for turbulent combustion include generally one or more high-power lasers for two-dimensional or pseudo three-dimensional measurements. The increased knowledge in chemical reactions in practical systems makes quantitative Planar Laser Induced Fluorescence possible and typical strategies as well as results have been recently reviewed in (Schulz and Sick, 2005). However, the complexity of such systems makes it inadequate for turbulent combustion sensing. Therefore, easier systems should be sought that can provide real-time information within the combustion systems. Those systems should add little complexity and among all be reliable. Recently, an extensive review has been proposed (see Docquier and Candel, 2002). It is known that the coupling between pressure and heat release will add energy to the instabilities, due to the pioneer work of Rayleigh. Therefore, for ACC, pressure sensor should be coupled with another sensor, possibly showing the behavior of the heat release as one deals with thermo-acoustics instabilities. The present research focused mainly on two sensors and detailed information on them will be presented in the next sections, especially focusing on their contribution to the oscillating combustion domain. The first one is the chemiluminescence emission for qualitative understanding of the flame dynamics and the second one is temperature measurement using DLAS technique. For each sensor, a brief specific introduction will be given and then the focus will be on the approach chosen to deal with the sensor and the latest results obtained. Diode-laser absorption of H_2O has been applied for the monitoring of a swirl-stabilized combustor (0.2MW) with secondary fuel injection. The availability of the diode-laser absorption for detection of high frequency combustion oscillation and combustion noise is investigated.

2. Chemiluminescence

2.1. Introduction

In many situations, one would like to understand the flame dynamics. The best solutions are based on laser

diagnostics that allow a critical discussion of flame front movement and position as well as velocity fields (see Tanahashi *et al*, 2004 for instance). However, for many practical cases, this is not possible due to the complexity of the experimental setup required and to the low time resolution. Therefore, one has to look for easier diagnostics that would however be able to provide information on flame dynamics. One of the easiest tools available in combustion diagnostics is the chemiluminescence. This is the light spontaneously emitted by some radicals created through chemical reaction. In many situations, three main species can be easily detected, OH* ($A^2\Sigma^+$-$X^2\Pi$), CH* ($A^2\Delta$-$X^2\Pi$) and C_2*($d^3\Pi_g$-$a^3\Pi_u$). It is known that however under high-pressure conditions, CO_2* emission will become important and practically covering all other species emissions (Docquier et al. 2002). The present target being atmospheric lean premixed combustion, it is still possible to use chemiluminescence emission as a reliable diagnostic tool. As lean premixed flames are taken, CH* and C_2* may not be very easily detectable. For the main mechanisms involved and the creation of excited radicals and in their de-excitation process, one may refer to (Kojima *et al*, 2005) who presented comparison between experimental results and numerical simulation using Chemkin mechanism for laminar-premixed flames. The next part deals with the application of chemiluminescence diagnostics in a combustor, prone to thermo-acoustics instabilities. There exists mainly two ways to gather chemiluminescence. The first is to use some collecting optics that would limit the field of view of the receiver and therefore allow only light emitted within a confined region to be used. The other way is to take all light, using a simple optic fiber, eventually coupled to a lens (see Docquier *et al.*, 2002). Both approaches are used for different purpose in the present study. Furthermore, to actually measure the signal, one may either use a spectrometer that would give within a range of wavelength the emission for each wavelength. This is a very accurate method but typical time response may be very limited. The other way is to use a series of photo-multipliers and mirrors to have time series data. Both approaches are used in the next sections and typical advantages are shown.

2.2. Presentation of the test rig

A short introduction of the test rig used is presented here. For more details, one may refer to (Tachibana et al., 2005). The main emphasis is on the sensors. A schematic figure of the test rig is shown in Fig. 1 as well as the structure of the injection system. All dimensions are given in mm. The main modification compared to previously tested injector (see Tachibana *et al.*, 2004) is the actual recess of 20mm.

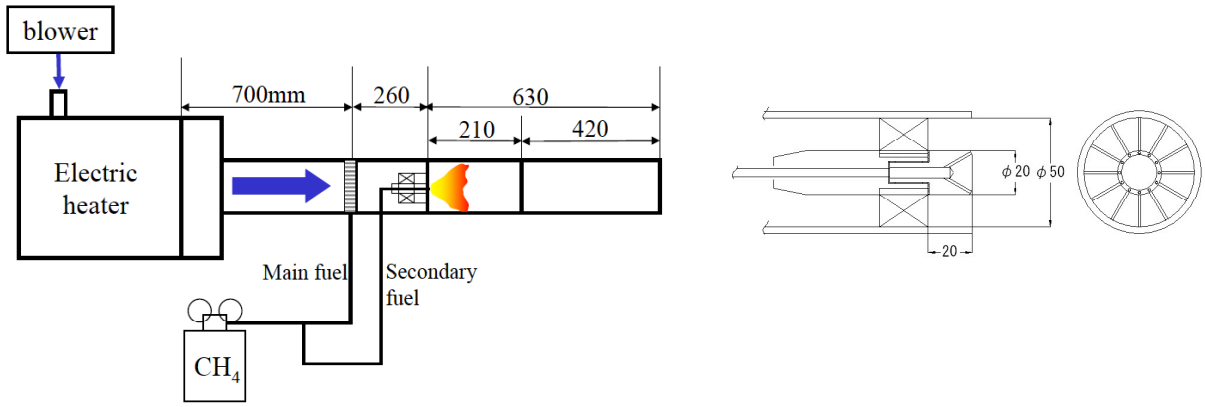

Fig. 1 Schematic of combustion rig

The typical inlet temperature is 700K with 90 $m.s^{-1}$ inlet velocity based on the swirl inlet area. This corresponds to a mass flow rate of 78g/s for the air (or a total flow rate of 1500 Nl/min). The overall equivalence ratio studied varies between 0.43 to 0.60, and the adiabatic temperature between 1660 to 1960K. The first part of the combustor (up to 210mm downstream the swirl) is composed of four quartz to allow complete optical access. The second part (420mm long) is water-cooled stainless plate. The chemiluminescence measurements have been taken in the first section, using either a simple fiber to get complete view of the section or a dual lens system in order to spatially limit the zone of interest. Both approaches provide slightly different data and they are examined in the next sections. Some results presented here do not include all details, as presented in other papers within this volume. The pressure sensor signal (Kulite Semiconductor Products, Inc., Model XTL-190-15G, located 10cm from the exit of the swirl) and time series chemiluminescence are acquired simultaneously through a multi-channel data acquisition system (ONO SOKKI, DS-200, Graduo). Typical sampling frequency is 25.6kHz for each channel. Each time it is necessary, the proper article will be referred. The pilot injection is referred as percentage versus the total fuel injected. If one refers to the main mixture's injection, this would lead to a value of 0.2%.

2.3. Spectrally resolved chemiluminescence

Spectral analysis of the flame offers very easy but however very fruitful information on the combustion mode. It is known that lean premixed combustion will mainly create OH* radicals and that radicals such as CH* and C_2*

will be very limited. To illustrate the lean premixed behavior, mean spectra are taken within oscillating combustion. The spectrometer used is the MS257 from Oriel coupled to an ICCD from Andor technology (DH534-18F-03 1024x0124 pixels). The ICCD is used in gate mode with an exposure of 60μs (which corresponds to values lower than 6° for oscillating combustion), intensification of 255 and a slit of 150μm. Full vertical binning is performed and accumulation over 1,000 samples is taken for each point. For those measurements, a series of two lenses was used. The lens was placed perpendicular to the combustor with a focal point in the center of the combustor, 10cm in the streamwise direction as well as in the transverse direction from the center. The fact that mainly OH* is visible for lean premixed combustion is perfectly shown in Fig. 2, for which the overall equivalence ratio taken was fixed at 0.50, without any pilot. The absolute value of the intensity of the signal is not taken into account and therefore only a relative intensity is shown on the left axis. One can notice the OH* peak around 306nm and one may distinguish around 431nm a secondary peak, induced by CH* radicals, even though its value above the background is not very intense. C_2* radicals are not visible for such lean conditions. On the other hand, looking at controlled cases through a secondary injection of fuel, one can notice the appearance of strong CH* (431nm and 387nm) and C_2* emission (around 473 and 516nm) as shown in Fig. 3. This is a clear indication of the diffusion type flames produced by the injection of the pilot. This may has, as a consequence, strong effects on nitrous oxide emissions and therefore, for completing active control schemes, it is important to check the possible increase in NOx levels induced by this diffusion flame.

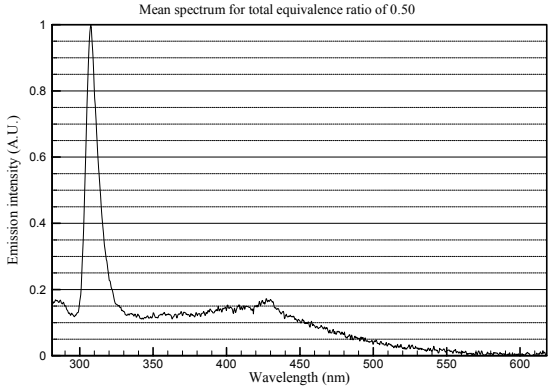

Fig. 2 Typical spectra for lean premixed flame (ϕ=0.50)

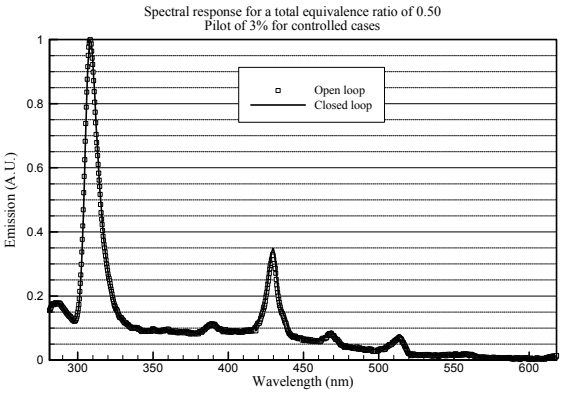

Fig. 3 Typical spectra when using active control

For active combustion, one may look more for temporal information to see changes within the combustor. Therefore, the next part presents typical temporal results obtained.

2.4. Time resolved chemiluminescence

Based on the previous results, one may think about using a series of band pass filter and photo multipliers to record the chemiluminescence emission of both OH* and CH*. The first band pass filter will be centered on 308nm and have a bandwidth of 10nm. This will enable the measurement of OH* emission, the second will be based on 431±2nm for CH* measurements. Similar experimental setup has already been used to propose criteria for offset of strong coupling between pressure and heat release (see Zimmer and Tachibana, 2004). Control using time series data of one chemiluminescence species has already been shown (see Paschereit *et al.*, 1998) for instance. To emphasize the relationship existing between chemiluminescence and pressure in an oscillating combustion case, one may compute the power spectrum density for both quantities. The acquisition frequency was set to 25kHz for the pressure and 20kHz for the chemiluminescence. The Sound Pressure Level can be computed with a reference of 20μPa, but for the chemiluminescence, the unity will be arbitrary as based on voltage. For lean flames, it is better to monitor OH* emission, as the signal to noise ratio is higher than any other species, as explicitly shown in Fig. 2. Typical results are presented in Fig. 4 for pressure based spectra and Fig. 5 for OH* based spectra. Each spectrum is based on the analysis of 30s acquired at 25kHz with 16384 points for each segment and an overlap of 50%.

Three cases are shown for both cases. One concerns strong oscillations (as shown by the sound pressure level reaching 170dB) for an overall equivalence ratio of 0.50 without secondary injection; therefore no control is applied. The two others are for controlled cases with either open or closed loop control. Looking closer to each spectrum, one can notice some differences that provide further understanding to the actual instabilities. For instance, the OH* spectra will exhibit clearly secondary peaks near the main peak for “no control” cases. Those peaks may be induced by the interaction between the main oscillating frequency (250Hz) and a secondary frequency, much smaller (of the order of 20Hz, as exhibited on the pressure spectra). Those interactions, seen in the chemiluminescence spectra indicate that they do affect the combustion process. Similar results on the interaction between a low and high frequency in combustion have been also recently reported (see Uhm and Acharya, 2004). One can also see on the closed loop control case distinguish very clearly the secondary

frequency induced by the control itself (near 230Hz) that in terms of global chemiluminescence has a level close to the actual controlled frequency (290Hz). On the other hand, the peaks around 850Hz appearing on the pressure spectra are not visible at all on the chemiluminescence one. This shows that this oscillating mode has no effect on the combustion itself and that as far as combustion is concerned; the main frequency in the "no control" case is the 250Hz and its sub harmonics. The relative decrease in the power spectrum for OH* comes from the fact that the chemiluminescence tends to be more uniform in time for the two controlled cases. Indeed, typical fluctuations are around 10% for controlled cases compared to typically 65% for the non-controlled case are measured with the photo multipliers. This last value indicates that the flame has a clear periodic movement and phase-locked measurements can reveal the dynamics. As far as controller input is concerned, it has already been shown (see Zimmer and Tachibana, 2004) that it is possible to compute an estimation of the coupling between pressure and chemiluminescence and that if this value is higher than a threshold, strong oscillations are to be expected. The main drawback of chemiluminescence compared to pressure is that absolute values can not be achieved, as depending on too many parameters whereas absolute measurements of pressure is quite trivial and therefore to quantify the changes made through the control loop, one will always refer to the pressure levels.

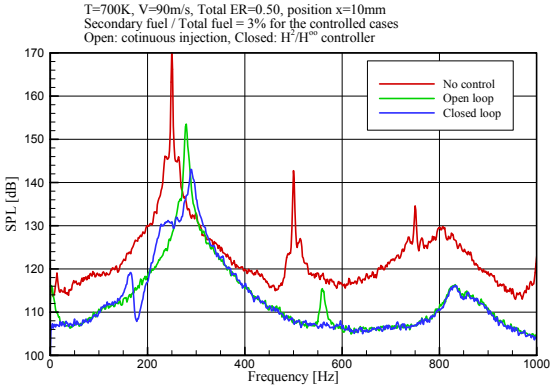

Fig. 4 Typical pressure based spectra

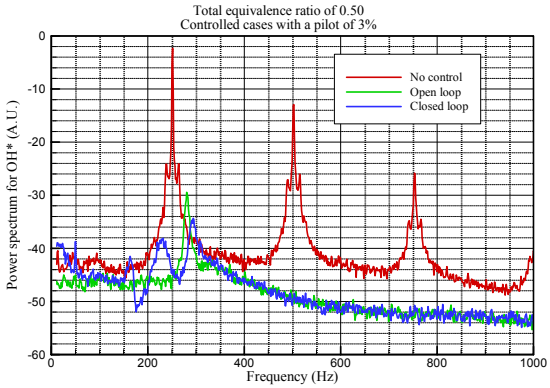

Fig. 5 Typical OH* based spectra

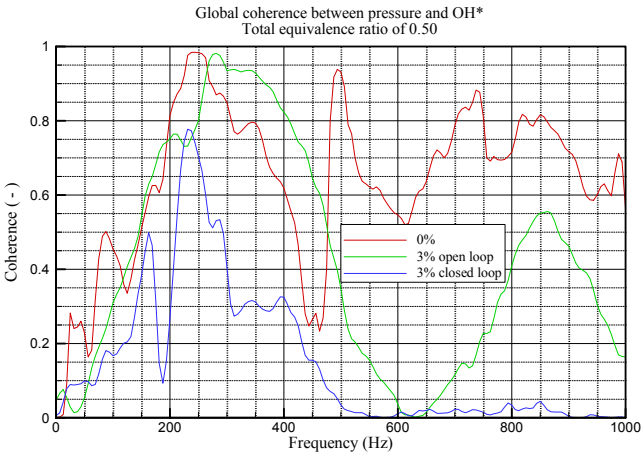

Fig. 6 Coherence between pressure and OH*

A further picture of the actual process inside the combustor can be obtained by computing the spectral coherence between the pressure and the chemiluminescence. This coherence will show the frequencies for which the coupling is strong and those for which the coupling is weak. This coupling is not be directly linked with the actual SPL for instance and therefore this provides a different information. Typical coherence between 10 and 1000Hz is shown in Fig. 6 for the three cases above. One can notice that for no control case, the coherence is very close to unity for a broad range of frequencies (between 230 and 260Hz), which means that pressure and chemiluminescence are well coupled in this frequency range. Using 3% for secondary injection does not really suppress the good coherence, but basically shifts it towards higher frequencies. This shift is due to a change in the adiabatic temperature of the total system, as the injected fuel is burning in a diffusion manner. The main changes however are for the secondary peaks (around 500Hz for no control case), which is not visible at all for the open loop case. Finally, as far as closed loop is concerned, one can clearly notice an overall lower coherence for the region between 250 and 300Hz (which is the peak region in SPL). This is an indication of the fact that closed loop puts out of phase pressure and chemiluminescence (therefore heat release). One can furthermore notice that higher frequencies do not lead to a coupling neither, whereas the open loop lead to a coherence of 0.50 for frequencies around 850Hz. However, one can notice that closed loop lead to a slight increase in the coherence around 230Hz, as already found in the power spectra (see Fig. 5). This is induced by the controller and may be a point of further improvement. This kind of approach helps understanding the role of control and strategies may be based on the monitoring of the coherence for instance.

2.5. Oscillating combustion characterization

To have a further insight of the dynamics, one may look at phase locked spectra and compute the relative levels

of OH*, CH* and C_2* in case of active control based on open and closed loop. The same experimental conditions as previously reported are used here again. For each condition, 16 points have been taken within one cycle, the spacing between each point is computed to fit the actual frequency occurring. The levels of the different chemiluminescence species are taken as being the integrated level simulating a bandwidth of 5nm around the peak. This is typically what is obtained when using a combination of photo-multiplier and band-pass filter. Furthermore, the background is also computed for each species independently so that the actual levels induced by the chemical species are measured. Both sides of the peak are used to determine a mean value of the background over a region of 5nm on each side. The evolution within one cycle is shown in Fig. 7 for the closed loop case. The left axis represents the chemiluminescence emission for each species. For clarity reason the results are plotted with a log scale. The X-axis represents the phase-delay with respect to the pressure signal. The maximum of emission in this case is obtained for a phase delay of 180° that corresponds to a zero level of pressure with a negative slope. Looking at the ratio of two different species (OH* and CH* in the present case) for both controlled case with closed and open loop, one can see, as shown in Fig. 8 that there exists a difference between the two situations. The relative variations of the ratio remain lower in the close loop case compared to the open loop one. A similar trend however is observed showing that the coupling may not be completely killed, but only damped by the closed loop scheme. This ratio does provide qualitative information but it is extremely difficult to deduce from those results some quantitative information. This phase-delay information is extremely important to understand the oscillations; as for instance a mean snapshot did not reveal any particular difference between the closed loop and the open loop case (see Fig. 3). In practical situations, this may be done very quickly as the acquisition of a typically 100 spectra for each phase delay and may be a part of the identification/control process.

It is also possible to look at the global emission and search for traces of periodic movement. In this case, the acquisition is triggered through the filtered pressure signal (around the proper frequency of oscillation) and the acquisition is set to 20kHz. To resample the point acquired on a phase delay grid, points within less than 6° of the desired phase delay are taken as representative of this phase. It is then possible to resample the grid without for instance using filters.

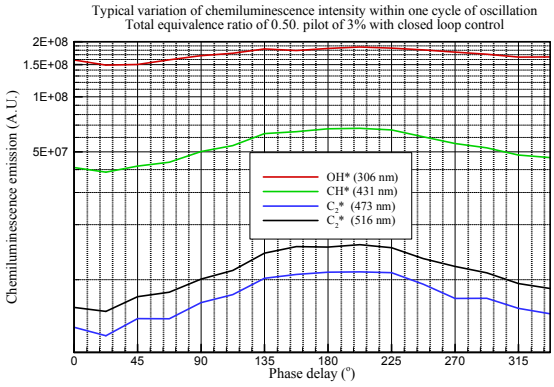

Fig. 7 Cyclic variation of chemiluminescence

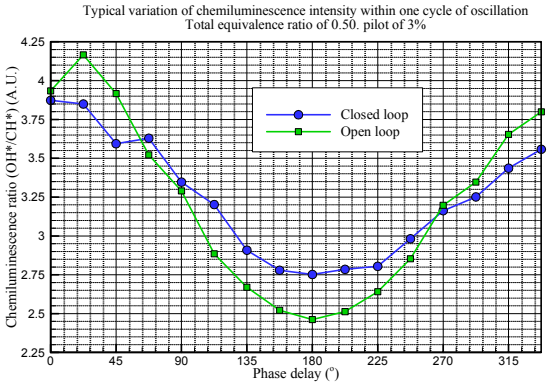

Fig. 8 Cyclic variation of ratio between OH* and CH*

Such results are shown for the three cases in Fig. 9 for the OH* radicals. For clarity reason, the controlled cases axis is given on the right and the uncontrolled one in the left. One can see clearly a sine shape for the uncontrolled case and for the open loop case, even though for this last one the amplitude is only limited to about 3% whereas the uncontrolled case lead to a peak to peak value of 50% of the mean value. Similar results may be obtained for the other species (like CH*). The interesting part is to compute relative ratio between two of the chemiluminescence species. Results are reported in Fig. 10.

The ratio reported is corrected to take into account the fact that the different photo multipliers have different voltage. The evolutions are presented as function of the phase delay, varying between 0 and 340°. One can first notice that the mean levels for controlled cases and the level of uncontrolled case differ. This may come from the influence of the pilot on the global chemiluminescence emission, because in this case, fully premixed combustion is not occurring and. The two controlled cases have values very close to each other, and those values do not have any sign of cyclic variation. Therefore, for controlled cases, the global ratio between OH* and CH* remains nearly constant within a cycle. On the other hand a clear periodic movement is seen for the uncontrolled case. Whereas the maximum of chemiluminescence emission was observed for a phase delay of 90°, the ratio between OH* and CH* has its minimum value for a phase delay of 150°. This phase delay corresponds to a pressure signal-crossing zero with a negative slope. The absolute value of this ratio can not be linked with the one presented in Fig. 8 as those previous ratio were obtained using the spectrometer and the present one using two photo-multipliers with different voltage. But it is interesting to see that close to the nozzle, fluctuations are detected whereas globally they are very limited. Similar results were obtained for the spectrometer for global monitoring of chemiluminescence, which indicates that, the present system of photomulitplers and mirrors gives qualitatively reliable results. Therefore, one may look for spatially limited chemiluminescence measurements to

have an insight of the injection of the methane and its effect on combustion (both from the main and the secondary). The monitored zone should be very close to the exit of the swirl, at the flame base. On the other hand global chemiluminescence provides information on the global stability of the system and its monitoring is useful for monitoring the changes induced by the thermo-acoustics instabilities on the dynamic of the flame.

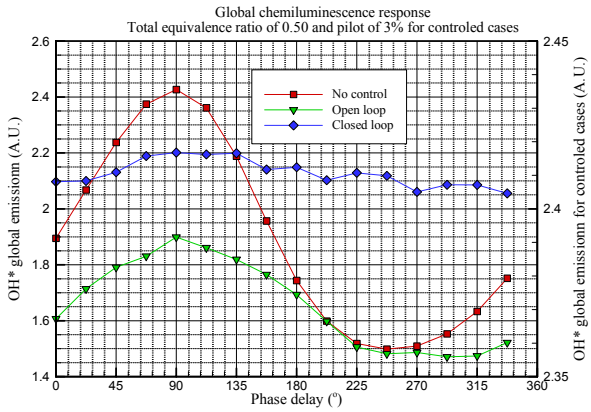

Fig. 9 Cyclic variation of global OH*

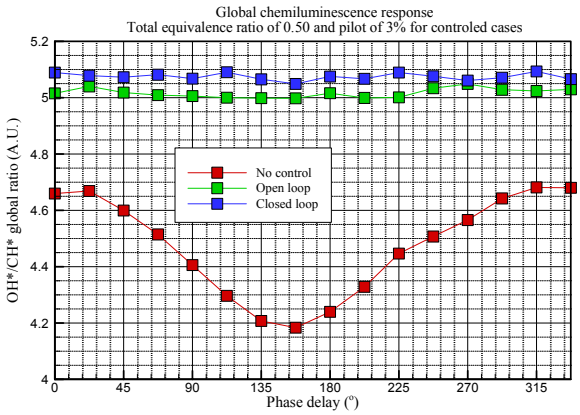

Fig. 10 Cyclic variation of global OH*/CH*

3. Diode laser

3.1. Introduction

Diode-laser absorption techniques have been developed for real-time monitoring of the combustion field (Arroyo, *et al.* 1993, Baer, *et al.* 1995, Furlong, *et al.* 1997). In the diode-laser absorption of the combustion field, absorption lines of molecule, which can reflect combustion condition of combustor, are used to measure temperature, mole fraction and velocity. In previous studies, diode-laser absorption techniques for H_2O (Baer, *et al.* 1995, Sanders, *et al.* 2000), CO (Webber, *et al.* 2000, Wang, *et al* 2000), CO_2 (Sonnenfroh, *et al.* 1997, Mihalcea, *et al.* 1998) have been developed. Since the system of the diode-laser absorption is relatively small and simple, it is a candidate of a sensor for monitoring combustion state of combustors in many engineering applications. For combustion controls, the diode-laser absorption have been used as a sensor in the Hencken burner (Furlong, *et al.* 1996, Furlong, *et al.* 1997), 50kW incinerator (Furlong, *et al.* 1997), 5kW dump combustor (Furlong, *et al.* 1998) and pulse detonation engine (Mattison, *et al.* 2003).

3.2. Experimental methods

Fig. 11 shows schematics of the multiplexed diode-laser absorption sensor system comprised of two diode lasers and fiber-optic components. This system uses scanned-wavelength laser absorption spectroscopy techniques. In the scanned-wavelength method, two lasers were current tuned by ramp-modulation across H_2O transitions near 1343nm ($\nu_1+\nu_2$ band) and 1392nm ($2\nu_1$ and $\nu_1+\nu_2$ bands).

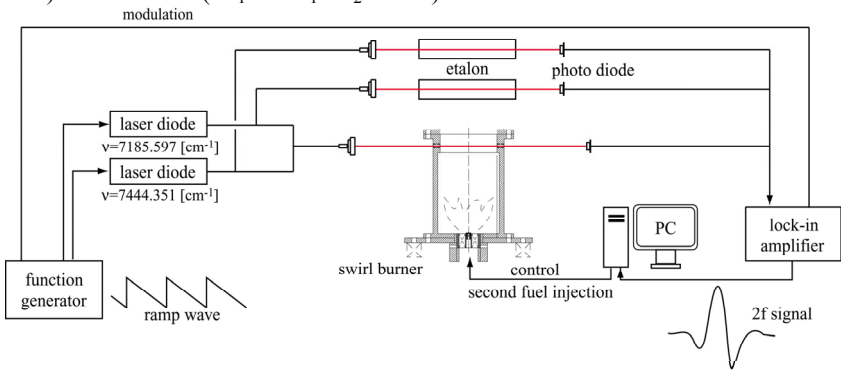

Fig. 11 Schematics of diode-laser absorption for the swirl-stabilized combustor (2*f* setup).

These wavelengths are widely used (Baer, *et al.* 1995), since line intensities of transition in these wavelengths are relatively high and independent of other species absorption spectra. The system usually uses the second-harmonic detection, but in the case of searching the combustor oscillation temperature and concentration of H_2O are inferred from directly measured absorption spectra. In this research, diode lasers are tuned at 2kHz repetition rate and directly detected to investigate combustion oscillation. The transmitted signal is recorded at a 1MHz sampling rate. Temperature of H_2O in burned gas is determined from the ratio of single-sweep integrated

line intensities, and mole fraction of H_2O is determined from measured line intensity and the calculated line strength at the measured temperature. In addition, this diode-laser system is available for the combustor oscillating over 1kHz frequency by using a fixed-wavelength laser absorption spectroscopy technique. In the fixed-wavelength method, the wavelength of each laser is fixed near the peak of each absorption feature. The transmitted fixed-wavelength laser signal is recorded at a 10kHz sampling rate.

3.3. Experimental apparatus and its characteristics

Fig. 12 shows the schematics of the swirl-stabilized burner and a direct photograph of methane-air turbulent premixed flame at stoichiometric condition with a flow rate Q=300 l/min. This combustion rig consists of a contraction section, a swirl nozzle section and combustion chamber. The inner diameter of 120mm in the contraction section is reduced to 40mm diameter. The swirl nozzle of 40mm inner diameter was mounted on the contraction section. The inner cross-section of combustion chamber was 120mm 120mm, and the length of the chamber was 550mm. On each side of combustion chamber, a silica glass plate of 120mm × 170mm and 5mm thickness was installed to allow optical access. The swirl nozzle has swirl vanes of 14mm inner diameter and 40mm outer diameter, inclined 45 degree from the nozzle axis. A secondary fuel nozzle was mounted at center of the swirl vanes. The premixed methane-air mixture pass through the swirl vanes and the flame was stabilized at swirl vanes as shown in the direct photograph.

In a previous study (Tanahashi *et al.* 2004, Choi *et al.* 2004), characteristics of the swirl-stabilized combustor have been investigated in details. It was shown that pressure spectrum has two distinct peaks near natural acoustic mode of combustor and beating of those peak frequencies is closely related with the combustion noise. For a case of ϕ=0.791 and 300 l/min, the sound level is about 110dB. If the secondary fuel is injected continuously, peak frequency of the pressure fluctuation changes, and r. m. s. of the pressure fluctuation is not affected by the secondary fuel injection. However, noise level reduces to about 100dB for an injection of 1% of secondary fuel compared to the total flow rate of the main mixture (which means that 11% of the fuel is issued through the secondary injection system and 89% through the main mixture). As for Q=300 l/min, the noise level could be reduced about 5dB more by controlling frequency of the secondary fuel injection. There is a most relevant frequency for the noise reduction found to be 40Hz for ϕ=0.791 and 300 l/min, where the equivalence ratio denotes the one of no control condition. Adding the 1% through the secondary injection system, the total overall equivalence ratio rises to 0.819. As for the sensor for the active control of the combustor; these characteristics of the combustor should be detected. It should be noted that the lean limit of this combustor has been extended to 0.2 without the increase of NOx production by the secondary fuel injection.

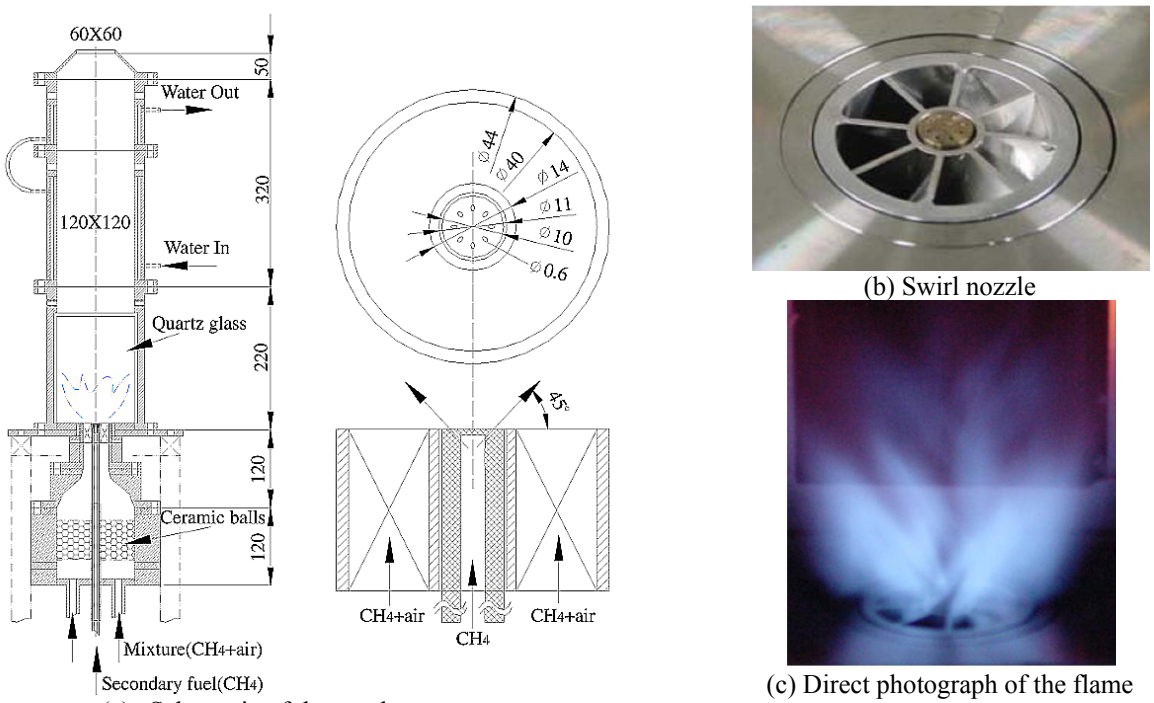

(a) Schematic of the combustor

(b) Swirl nozzle

(c) Direct photograph of the flame

Fig. 12 Schematics of combustion system and details of swirler and secondary fuel nozzle

3.4. Combustion monitoring by the diode-laser absorption

Fig. 13 shows transmission of two diode laser beams obtained for ϕ=0.791 and 300 l/min with no secondary fuel injection. In this measurement, ramp-wave frequency was set to be 2kHz and sampling was conducted with 1MHz. Since the transmission signals show distinct absorption, temperature and mole fraction of H_2O were

estimated from directly measured absorption spectra. Each time-dependent transmission signal is normalized by the incident laser intensity (Lambert-Beer relation) and transformed to a frequency-dependent line shape using information obtained from etalon fringe signal. Integrating absorbance leads to the line intensity, and temperature is estimated from the ratio of integrated line intensities. Note that it is impossible to determine accurate temperature and mole fraction since Lambert-Beer relation assumes that lasers should pass through a homogeneous media.

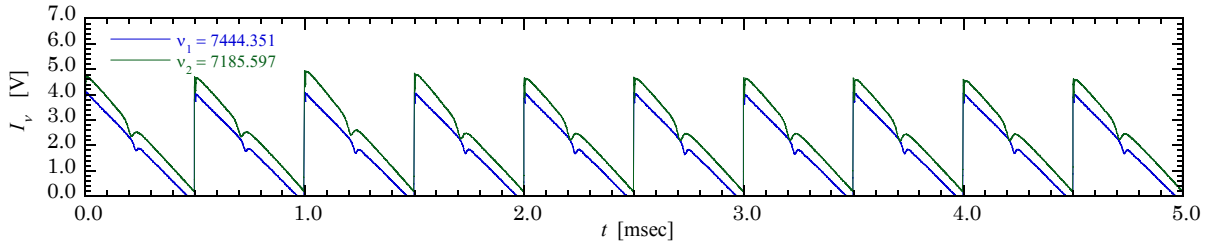

Fig. 13 Transmission of two diode laser beams with 2kHz ramp-wave frequency and 1MHz sampling frequency.

Fig. 14 shows estimated temperature and mole fraction of H_2O in the burned gas for no control case. The measured temperature and mole fraction shows relatively high frequency fluctuation in time.

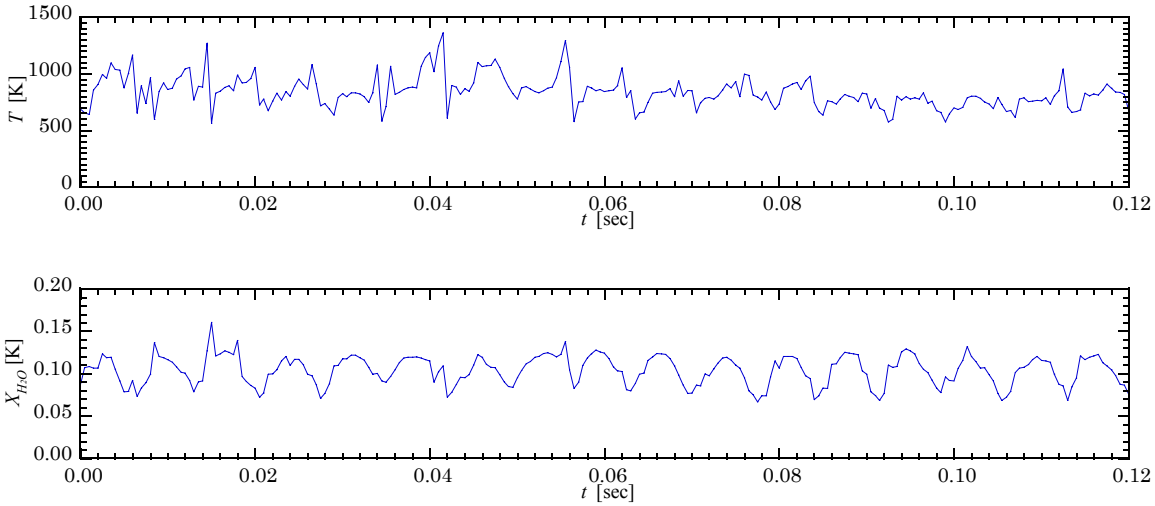

Fig. 14 Temperature and H_2O mole fraction obtained by diode laser absorption with 2kHz at the exit of the swirl stabilized combustor (no secondary fuel injection).

Table 1 denotes mean temperature and mole fraction obtained by absorption measurements for no control case, continuous secondary fuel injection case and frequency-controlled secondary fuel injection cases with 10Hz, 40Hz and 70Hz. For the no control case, space- and time-mean temperature measured by thermo-couple was 930K. The temperature difference between the absorption measurement and the thermo couple is approximate 80K, which suggests that, even in the inhomogeneous field such as the exhaust of the turbulent combustor, diode-laser absorption measurement can provide mean temperature and mean mole fraction approximately. For the case of the secondary fuel injection, mean values tend to increase because total equivalence ratio increases by the addition of pure fuel. Sound level depends on the frequency of the secondary fuel injection (Tanahashi *et al.* 2004) and become minimum at 40Hz, whereas mean temperature and mole fraction do not reflect this characteristics.

Table 1 Effects of secondary fuel injection on mean temperature and H_2O mole fraction.

Condition	No injection	Continuous	10Hz	40Hz	70Hz
$\langle T \rangle$ [K]	855.6	929.2	993.0	963.5	956.8
$\langle X_{H2O} \rangle$	0.0976	0.107	0.115	0.109	0.111

Fig. 15 illustrates standard deviation of time series temperature and mole fraction. On injecting secondary fuel, compared with the no control case, r. m. s. value for secondary fuel injection cases is reduced significantly. This may indicate noise level reduction. However, systematic difference in r. m. s. values of signals is not observed for different injection frequency cases.

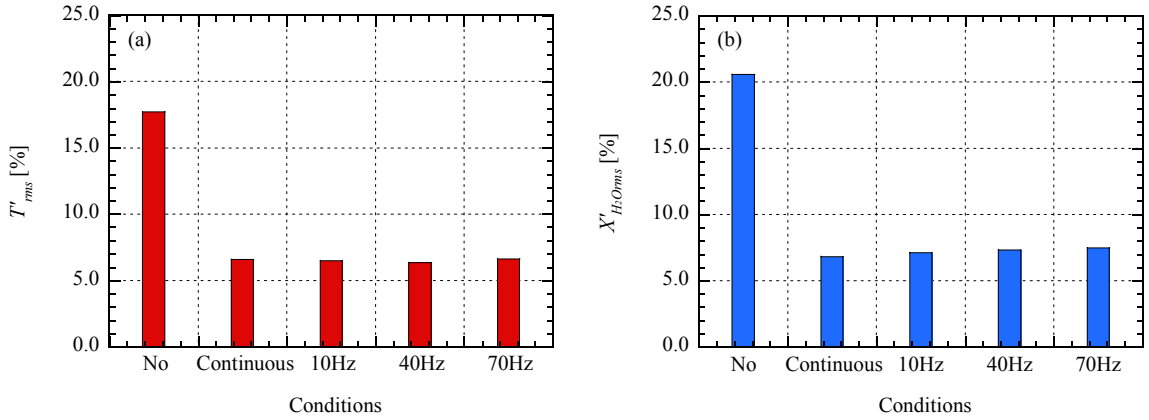

Fig. 15 Standard deviations of temperature (a) and H_2O mole fraction (b) on each secondary fuel injection conditions

Fig. 16 shows power spectra of temperature and mole fraction of H_2O. In temperature and mole fraction power spectra, by adding 40Hz secondary fuel injection, energy in 35Hz and 140Hz, which are peak frequency for no control case, are reduced drastically and high frequency components decay rapidly. Especially at 40Hz secondary fuel injection, energy in all range of frequency is reduced.

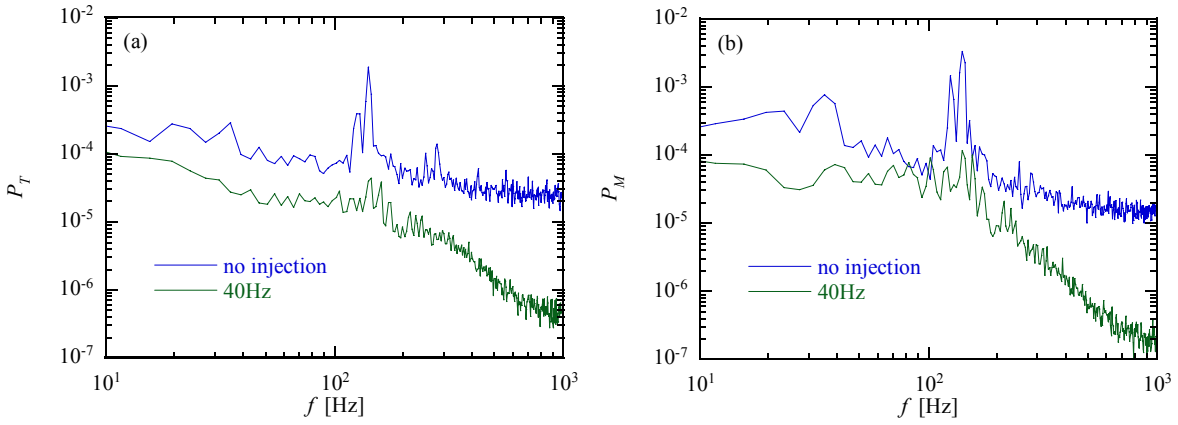

Fig. 16 Power spectra of temperature (a) and H_2O mole fraction (b) obtained for no secondary fuel injection and 1% secondary fuel injection under 40Hz-frequency control.

For the other frequency control cases, energy in 140Hz is not reduced sufficiently or a new peak arises. These characteristics can be related to the maximum noise reduction at 40Hz secondary fuel injection. Consequently, the diode-laser absorption can detect high frequency combustion oscillation and combustion noise by monitoring the r. m. s. values of temperature and H_2O mole fraction and energy level at peak frequency. Fig. 17 shows power spectra and r. m. s values obtained from the transmitted signals of the fixed-wavelength laser recorded at a 10kHz sampling rate.

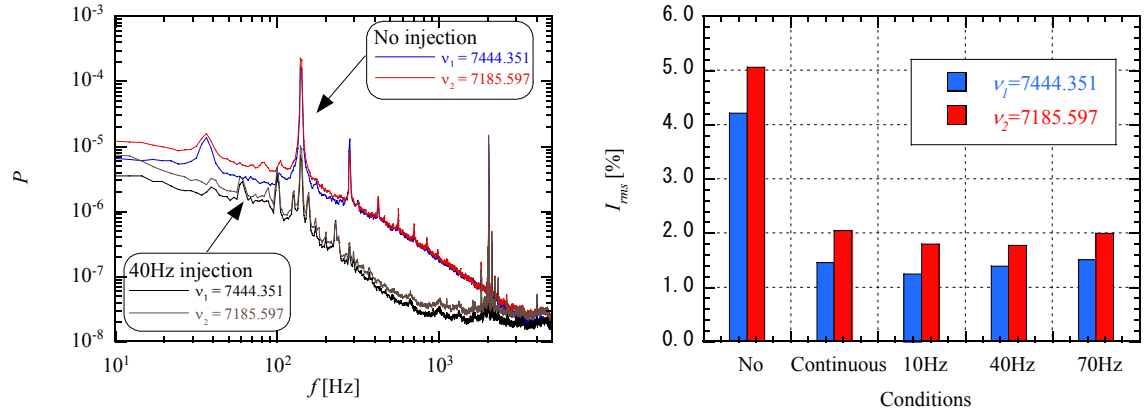

Fig. 17 Power spectra and standard deviations of transmitted signals on each secondary fuel injection conditions.

The power spectra and the standard deviations in the fixed-wavelength method are similar to those in the

scanned-wavelength method. So they infer combustion oscillation and noise even if the values are analyzed from the transmitted signals. In principle, it is possible to measure temperature and H_2O mole fraction in fixed-wavelength method, but in order to investigate higher frequency combustion oscillation and combustion noise it is necessary to use transmitted signals directly. It should be noted that 2*f* setup in Fig. 11 is more suitable for controls of large-scale combustors such as furnace.

4. Conclusions

The application of chemiluminescence sensor showed clearly differences between localized and global measurements. Using secondary injection of fuel for active control requires a monitoring of the neighborhood of the injection system to see the modifications induced and to allow an explanation of the actual decrease in pressure sound levels. On the other hand, a global monitoring reveals clearly strong fluctuations of chemiluminescence and its ratio when coupling between pressure and heat release is important. A control strategy tends to limit those global oscillations, limiting therefore heat release fluctuations. Furthermore, in this study, scanned- and fixed- wavelength diode laser absorption sensor system is applied to a swirl-stabilized combustor and used to detect high frequency combustion oscillation and combustion noise. From the power spectra and r. m. s. values of temperature and H_2O mole fraction obtained from scanned-wavelength method, the noise level reduction by secondary fuel injection can be detected. The results from the fixed-wavelength method show the same tendency with the scanned-wavelength method even if the transmitted signals are analyzed directly. These results suggest that the diode-laser absorption sensor is a strong candidate of a sensor for active combustion control purpose.

5. References

Arroyo, M. P. and Hanson, R. K. (1993), *Appl. Opt.* **32** , 30: 6104-6116.
Baer, D. S., Nagali, V., Furlong, E. R. and Hanson, R. K. (1995), *AIAA Paper-95-0426*.
Candel, S., *Proc. Combust. Inst.* **29**:1–28 (2002).
Choi, G. M., Tanahashi, M. and Miyauchi, T. (2004), *Proc. Combust. Inst.* **30**, 1807-1814.
Docquier, N. and Candel, S.,(2002), *Prog. Energy Combust. Sci.*, **28**:107-150.
Docquier, N., Lacas, F., and Candel, S., *Proc. Combust. Inst.* **29**:139–145 (2002).
Furlong, E. R., Baer, D. S. and Hanson, R. K. (1996), *Proc. Combust. Inst.* **26**. 2851-2858.
Furlong, E. R., Mihalcea. R. M., Webber, M. E., Baer, D. S. and Hanson, R. K. (1997), *AIAA Paper-97-0320.*
Furlong, E. R., Mihalcea. R. M., Webber, M. E., Baer, D. S. and Hanson, R. K. (1997), *AIAA Paper-97-2833.*
Furlong, E. R., Baer, D. S. and Hanson, R. K. (1998), *Proc. Combust. Inst.* **27**: 103-111.
Kim, K., Lee, J.G. and Santavicca, D.A., (2002), *AIAA paper* #2002-4024.
Kojima, J., Ikeda, Y. and Nakajima, T., (2005), *Combust. Flame*, **140**:34-45.
Mattison, D. W., Brophy, C. M., Sanders, S. T., Ma, L., Hinckley, K. M., Jeffries, J. B. and Hanson, R. K. (2003), *J. Propulsion and Power* **19**, 4: 568-572
Mihalcea, R. M., Baer, D. S. and Hanson, R. K. (1998), *AIAA Paper-98-0237.*
Paschereit, C.O., Gutmark, E. and Weisenstein, W. (1998), *Proc. Combust. Inst.* **27**, 1817-1824.
Sanders, S. T., Jenkins, T. P., Baldwin, J. A., Baer, D. S. and Hanson, R. K. (2000), *AIAA Paper-2000-0358*
Schulz, C. and Sick, V., (2005), *Prog. Energy Combust. Sci.*, **31**:75-121.
Sonnenfroh, D. M. and Allen, M. G. (1997), *Appl. Opt.* **36**, 15: 3298-3300.
Tachibana, S., Zimmer, L., Yamamoto, T., Kurosawa, Y., Yoshida, S. and Suzuki, K., (2004), *Proc. The 5th Sym. Smart Control of Turbulence*, pp. 175-183.
Tachibana, S., Zimmer, L., Kurosawa, Y., Suzuki, K., Shinjo, J., Mizobuchi, Y. and Ogawa, S., (2005), Active control of combustion oscillations in a lean premixed combustor by secondary fuel injection *Proc. The 6th Sym. Smart Control of Turbulence*
Tanahashi, M., Murakami, S., Miyauchi, T. and Choi, G-M., (2004), *Proc. The 5th Sym. Smart Control of Turbulence*, pp. 75-84
Uhm ,J.H. and Acharya, S., (2004), *Combust. Flame*, **139**:106-125.
Wang, J., Maiorov, M., Jefferies, J. B., Garbuzov, D. Z., Connoly, J. C. and Hanson, R. K. (2000), *Sci. Technol.* **11**, 1576-1584.
Webber, M. E., Wang, J., Sander, S. T., Baer, D. S. and Hanson, R. K. (2000), *Proc. Combust. Inst.* **28**, 407-413.
Zimmer, L. and Tachibana, S., (2004), *Proc. The 5th Sym. Smart Control of Turbulence*, pp. 85-94